Nicaraguan volcanoes record paleoceanographic changes accompanying closure of the Panama gateway

Terry Plank Department of Earth Sciences, Boston University, Boston, Massachusetts 02215, USA, and Department of Geology, University of Kansas, Lawrence, Kansas 66044, USA
Vaughn Balzer Department of Geology, University of Kansas, Lawrence, Kansas 66044, USA, and Department of Geology, Oregon State University, Corvallis, Oregon 97331, USA
Michael Carr Department of Geological Sciences, Rutgers University, Piscataway, New Jersey 08854, USA

ABSTRACT

A major oceanographic event preserved in the Cocos plate sedimentary column survived subduction and is recorded in the changing composition of Nicaraguan magmas. A uranium increase in these magmas since the latest Miocene (after 7 Ma) resulted from the "carbonate crash" at 10 Ma and the ensuing high organic carbon burial in the sediments. The response of the arc to this paleoceanographic event requires near steady-state sediment recycling at this margin since 20 Ma. This relative stability in sediment subduction invites one of the first attempts to balance sedimentary input and arc output across a subduction zone. Calculations based on Th indicate that as much as 75% of the sedimentary column was subducted beneath the arc. The Nicaraguan margin is one of the few places to observe such strong links between the oceans and the solid earth.

Keywords: Nicaragua, volcano, geochemistry, sediment, uranium.

INTRODUCTION

The growth rate of the continental crust and chemical evolution of the mantle depend in large part on the balance between subducted input and volcanic output at subduction zones. Sediment subduction represents a loss of mass from the continents and a gain of exotic chemical components in the mantle. The recycling of sedimentary material back to the continents via arc magmatism, however, modulates these effects. Despite the importance to the evolution of Earth, few studies have attempted to balance mass or chemical components across subduction zones (Patino et al., 2000; Bach et al., 1998). Many difficulties arise in attempting such a mass balance. For example, marine sections near trenches have been well sampled by ocean drilling (e.g., Rea and Ruff, 1996; Plank and Langmuir, 1998), but several million years of subduction separate these materials from those currently contributing to the magma-genesis zone, typically >100 km beneath the arc. This delay of a few million years is inherent to the recycling problem. Can we make sensible predictions about the material flux to depth, and/or can we assume that some aspects of the system are in steady state?

Previous work on the temporal variation of Western Pacific arcs has found that although some may respond to tectonic events such as backarc spreading (e.g., Tonga; Clift and Vroon, 1996), others have maintained a relatively constant geochemical composition for millions of years (e.g., Izu; Bryant et al., 1999). The sediment-recycling signature in these arcs, however, is weak and thus not ideal for exploring the temporal variability of sediment flux and delivery. However, sediment tracers such as the ^{10}Be abundance and the Ba/La ratio reach their global maximum in northwestern Nicaragua (Carr et al., 1990; Tera et al., 1986). Nicaragua also has the advantage that the arc has migrated trenchward with time; therefore, unlike other arcs where the volcanic history is buried by each successive eruption, the past >20 m.y. of arc volcanism is exposed in surface outcrops in Nicaragua (Ehrenborg, 1996).

TEMPORAL VARIATIONS IN COCOS PLATE SEDIMENTS

The other advantage to studying the temporal response to sediment subduction in Nicaragua is the simple sedimentary stratigraphy on the incoming Cocos plate (Fig. 1). Results from Deep Sea Drilling Project (DSDP) Leg 67 and Ocean Drilling Program (ODP) Legs 138 and 170 have provided a detailed history of sedimentation in the Guatemala Basin (Aubouin et al., 1982; Mayer et al., 1992; Kimura et al., 1997). The sedimentary column consists largely of two units, pelagic carbonate overlain by diatomaceous hemipelagic clayey ooze (Fig. 2). The boundary between these two units is roughly synchronous across the basin ca. 10 Ma and represents the "carbonate crash" (Lyle et al., 1995). The crash is thought to have been caused by an ~800 m rise in the carbonate compensation depth, apparently reflecting the cessa-

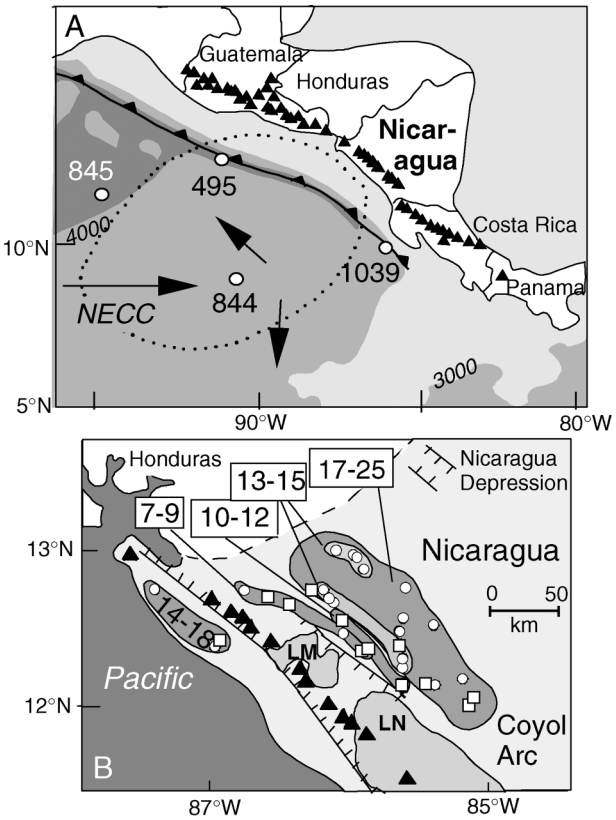

Figure 1. A: Central American volcanic arc (triangles) and Guatemala Basin (drill sites shown). Arrows indicate ocean circulation (North Equatorial Countercurrent, NECC). Dotted circle is high-productivity Costa Rica dome (drawn where thermocline shoals to ≤40 m in August–November; Fiedler et al., 1991). Shading is seafloor depth; contours are in meters. B: Volcanic arc in Nicaragua. Active volcanic front (solid triangles) and Miocene Coyol volcanic arc (open circles are samples dated by Ehrenborg [1996]; open squares are samples dated in this study). Age ranges are given in Ma. LN is Lago Nicaragua, and LM is Lago Managua.

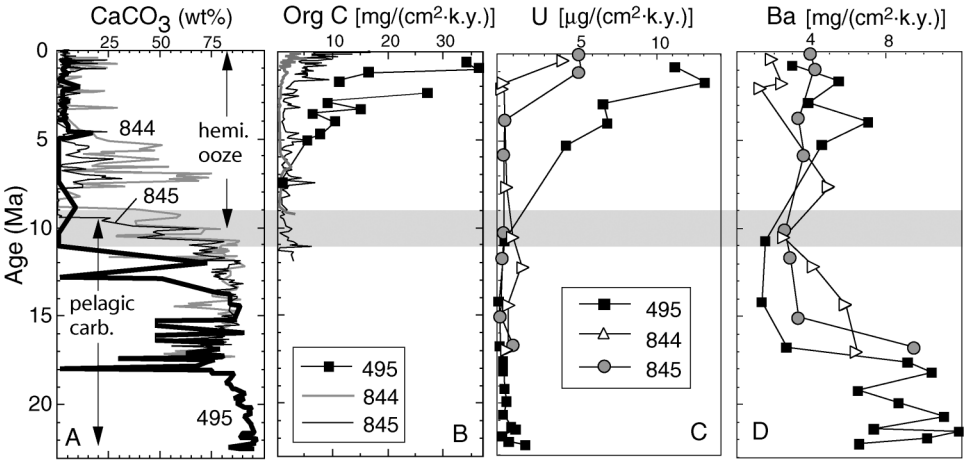

Figure 2. Lithostratigraphy and chemostratigraphy at Deep Sea Drilling Project Site 495 and Ocean Drilling Program Sites 844 and 845, Guatemala Basin. A and B: Calcium carbonate concentrations and organic carbon mass-accumulation rate downcore (Aubouin et al., 1982; Mayer et al., 1992). C and D: Ba and U mass-accumulation rate downcore. Site 495 data are from Patino et al. (2000); Sites 844 and 845 inductively coupled plasma–mass spectrometry data are in Data Repository (see text footnote 1). Shaded bar is 11–9 Ma time period of carbonate crash in Guatemala Basin and separates carbonate-rich from hemipelagic (hemi.) unit. High organic C and U at top of sections is most likely due to passage of sites beneath productive Costa Rica dome. Higher U concentrations at Site 495 are consistent with its longer history beneath dome.

tion of flow of less corrosive Caribbean intermediate and deep water into the Pacific following the shoaling of the Panama sill (Lyle et al., 1995; Farrell et al., 1995). Postcrash sediments were enriched in organic carbon as the seafloor approached the Costa Rica dome, a region of very high open-ocean surface productivity (Hofmann et al., 1981).

Because geochemical tracers are the means by which we detect sediment recycling, we need to relate the stratigraphic changes to changes in the geochemical fluxes into the trench. Toward this end, we analyzed 16 samples from ODP Sites 844 and 845 (Data Repository[1] and Fig. 2), which, when combined with data from DSDP Site 495 (Patino et al., 2000), provide a chemical stratigraphy of Guatemala Basin sediments. Although most elements have very different concentrations in the two lithologic units, we focus here on Ba and U, which are notably enriched in the modern Nicaraguan volcanic arc, where they correlate with unambiguous sediment tracers such as ^{10}Be.

The U abundance varies with lithologic type, being low in the lower pelagic carbonate unit (<500 ppb), but high in the upper hemipelagic ooze unit (to 10 ppm). As is commonly observed, U follows organic C owing to authigenic precipitation of reduced U(IV) oxides (Chase et al., 2001; Klinkhammer and Palmer, 1991). At face value, the steep increase in both organic C and U in the top 25 m of the columns might be expected as any site approaches land, receives terrestrial carbon, and then undergoes diagenetic release. There are several reasons, however, why this generic model does not appear to be the dominant control on the U and C distributions. These sites are at >3000 m water depth and far from coastal upwelling regimes and terrestrial carbon sources. This is consistent with C/N ratios in ODP Sites 844 and 845 sediments, which indicate predominantly marine sources (Meyers, 1997). The lack of sulfate reduction or ammonium production in pore fluids at ODP Sites 844 and 845 (Mayer et al., 1992) suggests that diagenesis may not be the major controlling process. Instead, the increase of U and organic C during the past few million years appears to coincide with passage of the sites beneath the increased productivity caused by upwelling in the Costa Rica dome (Fig. 1A). Although there is little direct information on the history of the Costa Rica dome, it likely strengthened ca. 5–4 Ma, when the shoaling of the Panama sill caused major changes in basin salinity (Haug et al., 2001), thermocline depth (Cannariato and Ravelo, 1997), surface currents (Nisancioglu et al., 2002), and position of the intertropical convergence zone (Hovan, 1995); the latter may have the largest effect on the formation and position of the dome (Hofmann et al., 1981).

Although high U at the top of the section seems to reflect high productivity in the Costa Rica dome, the low U abundances within the lower carbonate-rich unit are most likely due to a lack of preservation of organic matter. Carbonate-rich sediments typically have lower organic C abundances than clay-rich sediments. The reasons are debated, but the lower surface area of carbonate sediments, owing in part to the abundance of sand-sized foraminifera, may lead to poorly preserved organic C (Mayer, 1994; Pedersen, 1995) and by association, U. For example, ODP Sites 845 and 850 both underlie regions with similar modern surface productivity (Lyle, 1992), and yet the carbonate-rich surface sediments at Site 850 contain much lower organic C (<0.4 wt%) than the higher-surface-area clay-rich surface sediments at Site 845 (>2 wt% organic C). Thus, the U profile in the Cocos sediments reflects both biologic productivity and preservation. The closure of the Panama gateway led to the carbonate crash ca. 10 Ma and strengthened the Costa Rica dome ca. 5–4 Ma, both of which enhanced precipitation, preservation, and subduction of U in sediments at the Central American Trench.

In contrast to U, Ba accumulation rates were high prior to the carbonate crash and have decreased somewhat since. The entire column preserves a high proportion (>95%) of authigenic Ba (Schroeder et al., 1997), and the lithologic changes in the section appear to have had little effect on Ba preservation. High Ba concentration (>2000 ppm) is a long-term (>16 m.y.) feature of the subducting sedimentary column, whereas high U is not. Because mass-accumulation rates are directly proportional to subduction-input rates, high Ba accumulation translates into high Ba flux to the Central American Trench throughout the past 20 m.y., whereas the U flux has increased dramatically during the past several million years.

By using the foregoing inferences, we calculate sediment-subduction fluxes at 12 Ma, just prior to the carbonate crash, and at 2.5 Ma, the age of material currently beneath the arc (Table 1). These calculations show that the sedimentary flux of U to the trench has increased by a factor of 4, whereas the flux of Ba has varied only by ~10%.

SEDIMENT RECYCLING AT THE NICARAGUA ARC

In order to gauge the response of the Nicaragua arc to these temporal changes in the sediment input, we conducted a field campaign in 1996 to sample the Miocene Coyol arc (Ehrenborg, 1996; Fig. 1). The Ar-Ar dates (see footnote 1) range from 24 to 7 Ma, and the arc has migrated trenchward since ca. 13 Ma (Fig. 1). The unsampled 7–0 Ma

[1]GSA Data Repository item 2002128, Age data, geochemistry of sediments and volcanic rocks, and bulk sediment flux calculations, is available from Documents Secretary, GSA, P.O. Box 9140, Boulder, CO 80301–9140, editing@geosociety.org, or at www.geosociety.org/pubs/ft2002.htm.

TABLE 1. CONCENTRATIONS AND FLUXES

	U (ppm)	Th (ppm)	Ba (ppm)	La (ppm)	Material flux* ($\times 10^{10}$kg/m.y.)
Bulk sediment, 2.5 Ma	1.17	0.81	2705	14.0	2.8
Bulk sediment, 12 Ma	0.30	0.91	2422	13.5	2.9
Avg. Modern arc	0.69	0.89	663	6.9	3.3
Avg. Miocene arc	0.46	1.01	621	8.6	3.3
Fractionated MORB	0.14	0.37	28	7.8	

Note: MORB is mid-oceanic-ridge basalt. Sediment and Miocene arc concentrations are given in GSA Data Repository (see footnote 1 in text). Modern arc data from Carr and Rose (1987). Sediment column currently beneath Nicaragua was subducted at 2.5 Ma (on the basis of 68 mm/yr convergence rate, 68° slab dip, and 158 km depth to slab beneath arc). Arc flux calculated after subtracting mid-oceanic-ridge basalt (2× normal-MORB in Hofmann, 1988). Sediment flux at 2.5 Ma from 464 m column and 885.6 kg/m^3 dry bulk density. Sediment flux at 12 Ma from 454 m, 946.6 kg/m^3. Volcanic output rates from Patino et al. (2000); 1.17 × 107 m^3/Ma (per meter arc length) and 2800 kg/m^3 density.

*Per meter arc length.

volcanic section is presumably buried beneath volcaniclastic deposits in the Nicaragua depression. We collected ~60 samples (Balzer, 1999) and analyzed ~40 of the most mafic and least altered for major and trace elements and Sr isotopes (see footnote 1). In order to expand our coverage, we analyzed another ~20 samples collected previously (Nyström et al., 1988). The close similarities between the Coyol and modern arcs in major element and rare earth element (REE) compositions (Balzer, 1999) suggest that the Coyol volcanic rocks most likely represent the main Miocene arc, and not backarc volcanism.

Remarkably, the Coyol arc preserves the same along-strike trend in the Ba/La ratio as the modern arc, both in magnitude and spatial gradient (Fig. 3). This coincidence suggests that both the incoming flux of Ba and the delivery process have been fairly constant along this margin for 20 m.y. However, the Coyol arc is uniformly depleted in U relative to the modern arc (Fig. 3), a finding consistent with predicted stratigraphic changes in Cocos plate sediments. Because all the Coyol samples are older than 7 Ma and because the subduction time was ca. 2.5 Ma, the sedimentary columns contributing to the Coyol arc all preceded the carbonate crash. In addition to U and Ba, other chemical systematics are consistent with the predicted sedimentary fluxes. The Coyol and modern arcs are similar in their range of Ce/Pb ratios and Ce anomalies, as are the predicted sediment columns, whereas the Coyol arc has slightly lower $^{87}Sr/^{86}Sr$ ratios, as predicted from the global seawater Sr isotope curve. Thus, the temporal stability (in Ba, Ce/Pb, rare earth elements) and changes (in U and Sr isotopes) in the Nicaraguan arcs appear to originate in the oceanographic processes that control Cocos plate sedimentation.

Given the regularity in the subduction process at Nicaragua, it is possible to balance the input and output fluxes for some element tracers. A full mass balance would require an estimate of the composition of the subducting basaltic basement as well, because this layer also contributes elements to the arc (e.g., Elliott et al., 1997). Basaltic U buffers arc concentrations, which is the reason that the modern and Miocene arcs vary by at most a factor of two (Fig. 3), whereas the sediment flux varies by a factor of four (Table 1). Unfortunately, the Cocos basement has been poorly sampled in this region, so we focus here on the elements Th and Ba, the budgets of which in this arc are dominated by sediment input (Plank and Langmuir, 1993). We calculate (Table 1) that 76% of the sedimentary Th and 28% of the sedimentary Ba are recycled to the arc. These results are for the average Nicaraguan arc and do not take into account the large gradient in Ba/La ratio along the arc, which reflects important along-strike variations in delivery, the source of which is debated (Carr et al., 1990; Leeman et al., 1994; Herrstrom et al., 1995; von Huene et al., 2000). We obtain virtually the same mass balance for the 12 Ma sedimentary column and average Miocene arc (80% of the Th and 28% of the Ba), assuming a constant material flux for the arc. These calculations demonstrate near-steady-state recycling efficiency of this margin since 20 Ma. The preferential recycling of Th over Ba is not predicted from partition coefficients for red clay (Johnson and Plank, 1999), but may be related to the different behavior of the primary Ba host (sulfate) and Th host (silicate) in the subduction zone, or the shallow loss of Ba to a fluid during sulfate reduction (Shipboard Scientific Party, 1997). Regardless of the exact mechanisms, the magnitude of Th recycling requires subduction of at least 75% of the sedimentary column beneath the arc. This result is consistent with efficient ^{10}Be recycling (Tera et al., 1986), as well as the apparent lack of sedimentary accretion at the Nicaragua margin (Ranero and von Huene, 2000).

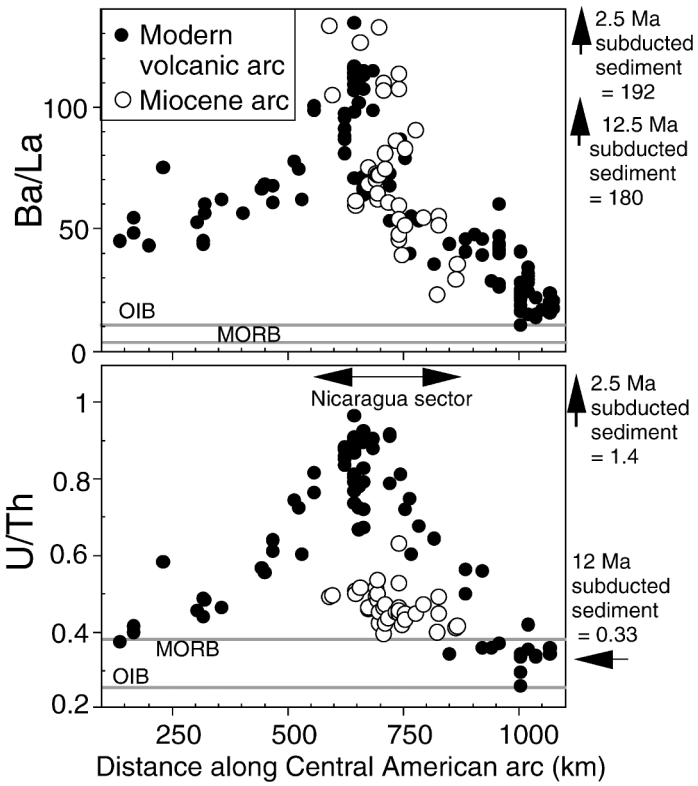

Figure 3. Geochemical variations along Central American volcanic arc, illustrating similar Ba/La ratios and contrasting U/Th ratios between modern and Miocene volcanic rocks in Nicaragua sector. These relationships are consistent with changes calculated for sedimentary columns subducted at 2.5 Ma and 12 Ma in Central American Trench (Table 1), shown as arrows (some off scale). Modern arc data are from Carr and Rose (1987); Miocene data are in Data Repository (see text footnote 1). Samples plotted have <53% SiO_2 (modern) or >3% MgO (Miocene), and <2% loss on ignition (least altered), and exclude high TiO_2 basalts (as in Carr et al., 1990). Alteration studies demonstrate that severe visible alteration (more than that for samples plotted here) leads to <6.5% U loss and 17% Ba addition (Balzer, 1999). U/Th and Ba/La ratios are plotted instead of U and Ba concentrations in order to minimize effects of partial melting and crystal fractionation and to distinguish from mid-oceanic-ridge basalts (MORBs) and oceanic-island basalts (OIBs). Average arc concentrations (no screening or normalizing) also reflect similar Ba (within 7%) and markedly different U (50%) between modern and Miocene arcs. Relationship between arc and sediment ratios is not 1:1 because ratios are fractionated as sedimentary material leaves subducting plate and mixes with mantle beneath arc.

The fidelity of the recycling process at the Nicaragua ''subduction factory'' illustrates how tectonic events reverberate through Earth. Tectonic uplift of the Isthmus of Panama restricted and ultimately ended communication between the tropical Atlantic and Pacific Oceans. This episode caused changes in seawater chemistry and ensuing sedimentation, which then affected element fluxes to the Central American Trench and ultimately the composition of magmas erupted in the vol-

canic arc. Although Patino et al. (2000) showed how the two sedimentary units on the Cocos plate can be resolved in eruptive products from a single volcano, we show how secular variations in the two units have been recorded in the arc during the past 20 m.y. It remains to be seen whether we can extend this treatment to volatile components and assess the impact of the carbonate crash and subduction cycling on the long-term global carbonate-CO_2 cycle.

ACKNOWLEDGMENTS

We thank J.-O. Nyström for generously providing Coyol arc samples and Wilfried Strauch and Nelson Buitrago at the Instituto Nicaraguense de Estudios Territoriales for help in Nicaragua. We also thank Rick Murray, Maureen Raymo, Andy Kurtz, Christina Ravelo, Simon Turner, and Mitch Lyle for discussions and reviews, Dan Gravatt for technical assistance, and Bruce Idleman at Lehigh University for performing Ar-Ar dating. Eli Silver, Kirk McIntosh, and Julie Morris were essential in the initiation of this project. We acknowledge support from U.S. National Science Foundation grants OCE-9521717 (to Plank) and EAR-9628251, EAR-9406624, and OCE-9521716 (to Carr).

REFERENCES CITED

Aubouin, J., and von Huene, R., 1982, Initial reports of the Deep Sea Drilling Project, Volume 67: Washington, D.C., U.S. Government Printing Office, 799 p.

Bach, W., Hegner, E., and Joerg, A., 1998, Chemical fluxes in the Tonga subduction zone: Evidence from the southern Lau Basin: Geophysical Research Letters, v. 25, p. 1467–1470.

Balzer, V.G., 1999, The late Miocene history of sediment subduction and recycling as recorded in the Nicaraguan volcanic arc [M.S. thesis]: Lawrence, University of Kansas, 151 p.

Bryant, C.J., Arculus, R.J., and Eggins, S.M., 1999, Laser ablation–inductively coupled plasma–mass spectrometry and tephras: A new approach to understanding arc magma genesis: Geology, v. 27, p. 1119–1122.

Cannariato, K.G., and Ravelo, A.C., 1997, Pliocene–Pleistocene evolution of the eastern Pacific surface water circulation and thermocline depth: Paleoceanography, v. 12, p. 805.

Carr, M.J., and Rose, W.I., Jr., 1987, CENTAM: A database of Central American volcanic rocks: Journal of Volcanology and Geothermal Research, v. 33, p. 239–240.

Carr, M.J., Feigenson, M.D., and Bennett, E.A., 1990, Incompatible element and isotopic evidence for tectonic control of source mixing and melt extraction along the Central American arc: Contributions to Mineralogy and Petrology, v. 105, p. 369–380.

Chase, Z., Anderson, R.F., and Fleisher, M.Q., 2001, Evidence from authigenic uranium for increased productivity of the glacial Subantarctic Ocean: Paleoceanography, v. 16, p. 468–478.

Clift, P.D., and Vroon, P.Z., 1996, Isotopic evolution of the Tonga arc during Lau Basin rifting: Evidence from the volcaniclastic record: Journal of Petrology, v. 37, p. 1153–1173.

Ehrenborg, J., 1996, A new stratigraphy for the Tertiary volcanic rocks of the Nicaragua Highland: Geological Society of America Bulletin, v. 108, p. 830–842.

Elliott, T., Plank, T., Zindler, A., White, W., and Bourdon, B., 1997, Element transport from subducted slab to volcanic front at the Mariana arc: Journal of Geophysical Research, v. 102, p. 14,991–15,019.

Farrell, J., Raffi, I., Janacek, T.R., Murray, D.W., Levitan, M., Dadey, K.A., Emeis, K.-C., Lyle, M., Flores, J.-A., and Hovan, S., 1995, Late Neogene sedimentation patterns in the eastern equatorial Pacific ocean, *in* Pisias, N.G., Mayer, L.A., et al., Proceedings of the Ocean Drilling Program, Scientific results, Volume 138: College Station, Texas, Ocean Drilling Program, p. 717–753.

Fiedler, P.C., Philbrick, V., and Chavez, F.P., 1991, Oceanic upwelling and productivity in the eastern tropical Pacific: Limnology and Oceanography, v. 36, p. 1834–1850.

Haug, G.H., Tiedemann, R., Zahn, R., and Ravelo, A.C., 2001, Role of Panama uplift on oceanic freshwater balance: Geology, v. 29, p. 207–210.

Herrstrom, E.A., Reagan, M.K., and Morris, J.D., 1995, Variations in lava composition associated with flow of asthenosphere beneath southern Central America: Geology, v. 23, p. 617–620.

Hofmann, A.W., 1988, Chemical differentiation of the Earth: The relationship between mantle, continental crust and oceanic crust: Earth and Planetary Science Letters, v. 90, p. 297–314.

Hofmann, E.E., Busalacchi, A.J., and O'Brien, J.J., 1981, Wind generation of the Costa Rica dome: Science, v. 214, p. 552–554.

Hovan, S., 1995, Late Cenozoic atmospheric circulation intensity and climatic history recorded by eolian deposition in the eastern Equatorial Pacific Ocean, Leg 138, *in* Pisias, N.G., Mayer, L.A., et al., Proceedings of the Ocean Drilling Program, Scientific results, Volume 138: College Station, Texas, Ocean Drilling Program, p. 615–625.

Johnson, M.C., and Plank, T., 1999, Dehydration and melting experiments constrain the fate of subducted sediments: Geochemistry Geophysics and Geosystems, v. 1, p. 1999GC000014.

Kimura, G., Silver, E., and Blum, P., 1997, Proceedings of the Ocean Drilling Program, Initial reports, Volume 170: College Station, Texas, Ocean Drilling Program, 554 p.

Klinkhammer, G.P., and Palmer, M.R., 1991, Uranium in the oceans: Where it goes and why: Geochimica et Cosmochimica Acta, v. 55, p. 1799–1806.

Leeman, W.P., Carr, M.J., and Morris, J.D., 1994, Boron geochemistry of the Central American volcanic arc—Constraints on the genesis of subduction-related magmas: Geochimica et Cosmochimica Acta, v. 58, p. 149–168.

Lyle, M., 1992, Composition maps of surface sediments of the eastern tropical Pacific ocean, *in* Mayer, L., Pisias, N., et al., Proceedings of the Ocean Drilling Program, Scientific results, Volume 138: College Station, Texas, Ocean Drilling Program, p. 101–115.

Lyle, M., Dadey, K.A., and Farrell, J.W., 1995, The late Miocene (11–8 Ma) eastern Pacific carbonate crash: Evidence for reorganization of deep-water circulation by the closure of the Panama gateway, *in* Pisias, N.G., Mayer, L.A., et al., Proceedings of the Ocean Drilling Program, Scientific results, Volume 138: College Station, Texas, Ocean Drilling Program, p. 821–838.

Mayer, L.M., 1994, Surface area control of organic carbon accumulation in continental shelf sediments: Geochimica et Cosmochimica Acta, v. 58, p. 1271–1284.

Mayer, L., Pisias, N., and Janacek, T., 1992, Proceedings of the Ocean Drilling Program, Initial reports, Volume 138: College Station, Texas, Ocean Drilling Program, 855 p.

Meyers, P.A., 1997, Organic geochemical proxies of paleoceanographic, paleolimnologic, and paleoclimatic processes: Organic Geochemistry, v. 27, p. 213–250.

Nisancioglu, K.H., Raymo, M.E., and Stone, P.H., 2002, Reorganization of Miocene deep water circulation in response to the shoaling of the Central American seaway: Paleoceanography (in press).

Nyström, J.-O., Levi, B., Troeng, B., Ehrenborg, J., and Carranza, G., 1998, Geochemistry of volcanic rocks in a traverse through Nicaragua: San Jose, Costa Rica, Revista Geologica de America Central, v. 8, p. 77–109.

Patino, L.C., Carr, M.J., and Feigenson, M.D., 2000, Local and regional variations in Central American arc lavas controlled by variations in subducted sediment input: Contributions to Mineralogy and Petrology, v. 138, p. 265.

Pedersen, T.F., 1995, Sedimentary organic matter preservation: An assessment and speculative synthesis: A comment: Marine Chemistry, v. 49, p. 117–119.

Plank, T., and Langmuir, C.H., 1993, Tracing trace elements from sediment input to volcanic output at subduction zones: Nature, v. 362, p. 739–743.

Plank, T., and Langmuir, C.H., 1998, The chemical composition of subducting sediment: Implications for the crust and mantle: Chemical Geology, v. 145, p. 325–394.

Ranero, C.R., and von Huene, R., 2000, Subduction erosion along the Middle America convergent margin: Nature, v. 404, p. 748–752.

Rea, D.K., and Ruff, L.J., 1996, Composition and mass flux of sediment entering the world's subduction zones: Implications for global sediment budgets, great earthquakes, and volcanism: Earth and Planetary Science Letters, v. 140, p. 1–12.

Schroeder, J.O., Murray, R.W., Leinen, M., Pflaum, R.C., and Janacek, T., 1997, Barium in equatorial Pacific carbonate sediment: Terrigenous, oxide, and biogenic associations: Paleoceanography, v. 12, p. 125–146.

Shipboard Scientific Party, 1997, Site 1040, *in* Kimura, G., Silver, E., et al., Proceedings of the Ocean Drilling Program, Scientific results, Volume 170: College Station, Texas, Ocean Drilling Program, p. 95–152.

Tera, F., Brown, L., Morris, J., Sacks, I.S., Klein, J., and Middleton, R., 1986, Sediment incorporation in island-arc magmas: Inferences from ^{10}Be: Geochimica et Cosmochimica Acta, v. 50, p. 535–550.

von Huene, R., Ranero, C.R., Weinrebe, W., and Hinz, K., 2000, Quaternary convergent margin tectonics of Costa Rica, segmentation of the Cocos plate, and Central American volcanism: Tectonics, v. 19, p. 314–334.

Manuscript received May 6, 2002
Revised manuscript received August 16, 2002
Manuscript accepted August 20, 2002

Printed in USA

Table DR1: Chemical analyes of ODP 844 and 845 sediments

Leg138-		844B	844B	844B	844B	844B	844B	844B	844B	845A	845A	845A	845A	845A	845A	845A	845A
Core-sec		2H-1	3H-2	4H-4	6H-6	9H-1	14H-4	21X-6	30X-6	1H-1	3H-5	7H-4	10H-2	16H-3	18H-5	25X-5	31X-4
cm interval		46-47	100-102	56-57	102-104	66-67	100-102	100-102	145-150	30-32	40-42	96-98	101-103	110-112	100-102	100-102	70-72
Subunit #		IA	IA	IB	IB	IIA	IIA	IIB	IIB	IA	IA	IA	IB	IIA	IIB	IIB	IIC
Depth (mcd)		6.1	18.76	20.02	55.13	80.32	138.8	212.14	299.21	0.31	24.37	65.43	94.6	162.44	185.89	258.74	314.34
Depth (mbsf)		4.96	16.5	28.6	51.03	71.77	124	193.5	280.6	0.31	23.51	60.6	86.1	144.71	166.61	233.51	289.11
Age (Ma)		0.45	1.82	2.05	7.74	10.53	12.18	14.41	17.07	0.0103	0.99119	3.87082	5.78568	10.2149	11.6704	15.0606	16.7506
ICP-ES:																	
SiO2		40.77	54.28	57.84	62.68	53.75	6.22	34.06	31.38	48.41	56.18	55.72	46.81	30.11	12.95	10.29	10.76
TiO2		0.421	0.640	0.527	0.403	0.053	0.009	0.008	0.017	0.379	0.427	0.543	0.387	0.118	0.062	0.029	0.057
Al2O3		8.18	12.89	13.04	7.55	1.18	0.36	0.37	0.44	8.46	9.66	11.94	8.75	3.67	0.84	0.79	1.09
Fe2O3		5.82	6.98	5.17	3.10	0.86	0.22	0.16	0.53	6.52	6.15	6.89	7.49	7.39	2.57	3.11	3.47
MnO		0.246	0.201	0.225	0.210	0.114	0.056	0.053	0.181	0.321	0.302	0.653	1.023	1.209	0.274	0.262	1.207
MgO		3.06	3.53	2.50	2.06	0.93	0.32	0.34	0.57	3.73	3.61	3.65	4.00	2.36	1.00	1.08	2.11
CaO		12.98	1.49	2.53	4.24	19.11	50.67	33.68	36.65	3.72	3.03	1.57	7.07	26.30	43.19	44.88	43.61
NaO		5.17	6.38	4.99	5.93	3.79	1.31	1.84	1.83	8.77	6.38	5.81	6.31	3.83	2.02	1.44	1.13
K2O		1.16	1.67	2.44	1.51	0.45	0.21	0.19	0.21	1.55	1.42	1.76	1.36	0.85	0.35	0.36	0.24
P2O5		0.187	0.262	0.236	0.224	0.136	0.089	0.045	0.048	0.174	0.171	0.365	0.402	0.430	0.151	0.177	0.189
LOI		21.53	10.56	9.70	11.03	19.00	40.23	28.91	27.81	17.37	11.86	10.16	15.45	22.93	36.15	37.21	35.76
H20-		8.36	15.31	8.11	10.01	8.89	3.01	4.30	3.56	15.90	14.92	14.43	12.31	9.33	4.45	3.34	5.13
Sr		554	434	369	563	830	1605	1091	1211	361	372	346	556	1197	1753	1502	1299
Ba		4285	10671	7634	10269	5361	1428	2378	2159	5578	7766	9094	8915	6998	2637	2254	2430
shipboard:																	
CaCO3 %		19.5	0.1	2.2	5.9	28.1	90.3	74.3	68.6	5.08	4.25	0.67	10.92	47.84	75.59	79.09	76.59
Org. C %		0.9	0.4	0.3	0.2	0.5	na	na	na	2.27	0.94	0.35	0.64	0.52	na	na	na
ICP-MS:	iso																
Li	7	45.43	59.96	46.20	18.08	10.76	4.01	1.64	10.32	39.14	50.27	55.32	45.27	21.48	8.92	10.50	40.63
Be	9	1.068	1.551	1.515	1.545	0.767	0.149	0.446	0.335	1.204	1.387	1.780	1.726	1.459	0.380	0.474	0.402
Sc	45	20.67	25.30	19.98	13.96	7.02	1.57	2.38	2.49	24.25	23.83	25.30	19.89	9.06	3.03	2.79	4.77
V	51	316.8	132.9	97.9	69.4	48.6	11.3	9.0	14.7	166.5	222.8	101.1	242.6	35.2	58.8	26.1	34.2
Cr	52	41.80	67.79	40.49	16.10	6.30	1.27	2.19	3.75	35.13	39.00	60.00	36.14	9.48	6.46	5.26	3.13
Co	59	67.19	49.72	32.03	41.33	7.28	2.49	3.47	3.85	39.18	50.92	78.22	74.12	19.91	4.43	5.78	7.41
Ni	60	704.0	480.4	260.2	422.2	111.0	10.3	10.2	10.5	445.1	486.7	573.7	706.6	77.8	20.9	26.4	32.1
Cu	63	336.1	303.8	410.5	241.9	145.8	32.4	223.5	44.0	299.0	444.2	1017.6	1415.0	271.6	119.5	81.5	149.6
Zn	66	503.3	451.9	233.5	267.7	128.6	20.8	20.9	21.7	608.3	579.3	405.9	505.0	148.5	41.0	54.6	65.6
Ga	71	12.67	21.85	17.86	13.42	3.33	0.94	1.56	1.30	13.85	17.35	22.22	16.03	10.05	2.10	1.94	2.11
Rb	85	27.05	43.50	69.71	31.59	5.38	0.93	1.18	2.68	34.93	37.26	46.85	41.46	42.58	7.65	8.69	5.36
Sr	88	558	441	376	570	817	1580	1078	1201	366	379	352	560	1159	1749	1478	1281
Y	89	34.1	65.1	59.5	48.1	22.2	11.5	8.2	8.8	38.1	41.3	80.6	95.4	64.6	26.5	17.6	20.8
Zr	90	85.2	150.7	151.2	128.8	40.6	7.4	15.9	12.2	109.9	111.5	131.4	121.2	78.3	19.4	18.9	21.5
Nb	93	4.584	7.908	7.755	8.067	0.853	0.163	0.173	0.354	4.537	5.108	6.139	5.325	3.989	0.524	0.570	0.887
Cs	133	1.813	2.475	3.484	1.020	0.180	0.033	0.036	0.085	2.232	2.649	3.030	2.136	1.907	0.240	0.218	0.123
Ba	135	4256	10505	7506	10157	5453	1450	2407	2178	5498	7626	8948	8855	7236	2643	2291	2466
La	139	16.73	30.89	32.73	25.32	9.93	3.65	3.23	3.96	21.47	21.88	41.92	55.11	39.84	12.49	8.32	11.40
Ce	140	25.02	38.65	46.14	31.69	4.54	0.84	0.89	1.44	27.23	29.97	42.49	36.35	22.91	3.76	3.08	3.84
Pr	141	4.00	7.75	7.99	6.32	2.11	0.60	0.62	0.81	5.16	5.62	10.80	12.48	8.77	2.40	1.60	2.55
Nd	146	16.96	33.08	32.50	26.48	9.11	2.64	2.67	3.46	21.73	24.00	45.98	52.90	36.46	10.35	6.88	10.74
Sm	147	3.86	7.34	6.88	6.15	1.95	0.53	0.57	0.73	4.74	5.42	10.28	11.19	7.17	2.08	1.41	2.26
Eu	151	1.059	2.034	1.781	1.715	0.335	0.152	0.131	0.177	1.291	1.466	2.731	2.980	1.638	0.545	0.373	0.594
Gd	160	4.593	8.787	7.787	7.118	2.55	0.81	0.79	0.98	5.596	6.328	11.961	13.574	9.08	2.84	1.93	2.83
Tb	159	0.797	1.533	1.352	1.222	0.431	0.140	0.134	0.170	0.978	1.099	2.064	2.297	1.557	0.481	0.329	0.485
Dy	162	4.66	8.88	7.77	7.02	2.58	0.89	0.80	1.00	5.60	6.26	11.60	13.12	9.11	2.85	1.95	2.75
Ho	165	1.057	1.991	1.724	1.558	0.590	0.222	0.186	0.226	1.237	1.359	2.498	2.895	2.013	0.645	0.447	0.592
Er	166	3.12	5.78	5.00	4.48	1.72	0.68	0.54	0.65	3.56	3.84	7.09	8.16	5.73	1.86	1.31	1.67
Yb	174	3.12	5.71	4.89	4.25	1.64	0.65	0.52	0.62	3.59	3.74	6.73	7.40	5.17	1.68	1.24	1.53
Lu	175	0.516	0.932	0.793	0.676	0.276	0.112	0.088	0.100	0.590	0.605	1.087	1.176	0.819	0.262	0.198	0.237
Hf	178	1.714	2.756	3.250	2.506	0.498	0.105	0.166	0.165	1.872	1.994	2.318	1.997	1.504	0.261	0.246	0.374
Ta	181	0.228	0.403	0.454	0.407	0.047	0.009	0.007	0.018	0.223	0.255	0.303	0.255	0.292	0.028	0.023	0.048
Pb	208	8.10	14.58	15.08	11.89	2.91	0.74	0.58	1.31	17.78	16.12	33.34	13.65	19.34	2.55	6.06	8.51
Th	232	2.259	3.108	6.250	2.910	0.347	0.052	0.066	0.118	2.754	2.715	3.283	2.860	3.746	0.271	0.210	0.273
U	238	9.651	1.508	2.125	1.232	1.986	0.541	0.272	0.232	7.074	9.668	1.330	0.956	0.996	0.260	0.104	0.267

Samples taken from same interval as shipboard carbon/carbonate measurements (Mayer et al., 1992); na: no analysis; mcd: meters composite depth;
mbsf: meters below seafloor; LOI: weight loss on ignition to 950°C; H2O-: weight loss to 105°C; all concentrations reported relative to dry (105°C) weight
ICP-MS solution were prepared in Savillex beakers as described in Johnson and Plank (1999), except H2O2 was added to decompose organic matter,
and HNO3 and HF were added sequentially to dissolve first carbaonte and then silicate in carbonate-rich samples
Unknowns were calibrated using volcanic rock standard reference materials, with Ca, Sr and Ba added to match carbonate matrix
68Zn, 69Ga, 139La, 147Sm and 151Eu were corrected for Ba intereferences
ICP-ES solutions were prepared by LiBO2 fusion, after Plank and Ludden (1992); see Balzer (1999) for further details on ICP-ES and ICP-MS analyses.

Table DR2: Chemical analyses, locations and ages of Miocene volcanics from Nicaragua

Sample	CHD 2	CHD 3	TAM 2	LEO 18	LEO 25A	LEO 25B	TAM 1	LEO 8	LEO 9	TOR 1	LAR 1LM
Split	Ny	Ny		Ny	Ny	Ny		Ny	Ny		
UTM E			538.9	506.7	537.8	537.8	538.9	538.6	539.4	530.4	544.9
UTM N			1341	1372.9	1342.6	1342.6	1341	1341.1	1340.5	1404	1405.1
Age (Ma)			16.28								
err			0.26								
Age gr.	II	II	II	II	II	II	II	II	II	I	I
Region	Tam	Tam	Tam	Tam	Tam	Tam	Tam	Tam	Tam	Lar	Lar
Dist. (km)	591	596	648	648	691	691	693	693	693	647	657
DCP-ES:											
SiO2	53.19	54.74	54.51	50.58	58.62	58.57	50.91	54.55	51.80	52.96	67.08
TiO2	1.11	1.18	1.50	1.38	1.15	1.26	1.30	1.50	1.06	1.71	0.58
Al2O3	16.32	16.41	15.54	16.43	14.52	14.75	17.28	15.11	18.70	17.29	16.59
FeO	10.32	10.29	11.83	12.14	10.41	9.90	11.55	11.98	10.40	9.05	4.05
MnO	0.18	0.19	0.21	0.20	0.23	0.25	0.21	0.24	0.20	0.13	0.09
MgO	5.53	4.51	4.12	5.73	3.16	3.32	5.52	4.24	4.17	4.92	1.31
CaO	9.75	8.72	8.47	10.28	7.45	7.89	10.12	8.23	10.22	9.09	4.07
Na2O	2.80	3.00	2.90	2.66	3.29	3.29	2.46	3.17	2.78	3.32	4.18
K2O	0.60	0.73	0.65	0.50	0.96	0.55	0.47	0.66	0.53	1.10	1.88
P2O5	0.19	0.23	0.26	0.08	0.22	0.22	0.20	0.33	0.13	0.43	0.17
LOI	0.59	0.86	0.11	1.41	0.45	1.00	1.49	0.75	0.49	0.99	1.38
ICP-MS:											
Li	9.32	10.02	13.97	8.03	23.59	7.02	8.32	12.09	5.83		4.54
Be	0.53	0.64	0.80	0.65	0.74	0.81	0.67	0.80	0.51		1.19
Sc	39.82	36.67	42.46	42.04	38.93	39.95	40.89	43.24	36.19	20.35	14.70
V	365.37	380.23	355.81	406.52	276.35	287.00	398.29	356.23	357.79	249.44	96.32
Cr	53.99	10.81	2.26	69.33	1.10	0.63	69.00	2.70	20.34	78.71	1.76
Co	34.22	31.60	34.24	38.53	25.52	26.45	37.84	32.88	31.00	30.50	7.83
Ni	21.71	13.02	8.39	30.85	2.34	2.04	30.60	7.29	12.93	36.35	2.96
Cu	231.56	344.49	266.34	353.37	178.83	174.10	294.18	269.79	202.42	149.89	30.96
Zn	96.55	101.94	124.18	110.80	119.78	124.51	110.66	122.80	96.34	127.04	65.65
Rb	10.31	11.72	6.07	8.33	7.26	4.95	6.75	4.06	5.10	6.29	48.63
Sr	370.03	377.09	312.32	332.04	323.62	369.35	332.95	305.62	355.93	1233.85	331.83
Y	23.75	27.72	39.55	30.94	34.15	37.38	29.50	39.72	21.96	13.18	40.10
Zr	65.06	85.69	99.84	81.85	91.14	93.86	77.25	102.60	53.01	56.50	168.88
Nb	0.97	1.77	1.64	1.62	1.46	1.50	1.50	1.62	0.91	3.18	3.26
Cs	0.37	0.20	0.06	0.61	0.06	0.64	0.38	0.05	0.09	0.19	1.98
Ba	477.63	515.40	387.12	297.03	433.43	478.35	285.04	421.80	272.92	661.20	1196.43
Ga	17.03	17.53	17.13	17.94	17.19	17.68	17.16	17.68	18.61		9.95
La	3.59	4.92	6.51	4.81	6.15	6.55	4.56	6.54	3.79	11.32	14.15
Ce	9.55	12.91	17.07	13.09	15.56	16.40	12.36	17.20	9.45	25.22	28.82
Pr	1.73	2.26	2.98	2.33	2.69	2.83	2.19	3.02	1.66	4.32	4.64
Nd	8.90	11.41	14.98	11.98	13.55	14.17	11.22	15.34	8.29	20.03	20.56
Sm	2.76	3.42	4.66	3.72	4.03	4.25	3.57	4.68	2.51	4.37	5.19
Eu	0.99	1.16	1.55	1.28	1.38	1.44	1.20	1.55	0.94	1.59	1.40
Gd	3.54	4.27	5.86	4.76	5.09	5.41	4.50	5.91	3.22	3.74	6.02
Tb	0.67	0.80	1.09	0.88	0.96	1.01	0.83	1.10	0.60	0.56	1.07
Dy	3.91	4.63	6.41	5.19	5.65	5.98	4.90	6.48	3.55	2.66	6.07
Ho	0.84	0.99	1.40	1.12	1.22	1.31	1.05	1.40	0.78	0.46	1.30
Er	2.40	2.83	3.94	3.18	3.48	3.72	3.00	3.97	2.23	1.19	3.76
Yb	2.34	2.77	3.79	3.06	3.41	3.62	2.90	3.83	2.18	0.95	3.91
Lu	0.37	0.44	0.61	0.48	0.54	0.58	0.46	0.61	0.34	0.15	0.65
Hf	1.92	2.49	2.86	2.39	2.65	2.73	2.20	2.93	1.53	1.77	4.15
Ta	0.07	0.12	0.11	0.11	0.11	0.11	0.10	0.11	0.06	0.20	0.23
Pb	2.90	3.28	3.44	3.29	3.66	4.05	2.78	3.72	2.27	3.72	6.70
Th	0.28	0.42	0.54	0.41	0.60	0.62	0.39	0.56	0.20	0.25	2.07
U	0.14	0.21	0.28	0.20	0.30	0.32	0.19	0.28	0.11	0.12	0.97
$^{87}Sr/^{86}Sr$											

Oxides (wt%); Elements (ppm). Ny = Splits from Nystrom et al. (1988); Ar-Ar total fusion groundmass ages, Lehigh Univ. Age group I ~ 6-13 Ma, II ~ 16-24 Ma; (*) = step heating Ar-Ar ages. Regions: Tamarindo, Larreynaga, Zarzales, Ciudad Dairo-Laguna Mayua, San Jacinto- Las Lajas, San Lorenzo, San Esteban, Juigalpa, El Rama. Major elements by DCP-ES at Rutgers University; and ICP-ES at the University of Kansas for Ny splits. All Fe calculated as FeO, and major elements summed to 100%. Trace elements by ICP-MS at University of Kansas. ICP-MS precision is better than 3% based on replicate analyses of a basalt standard (MAR) over the course of this project. Analytical procedures followed those in Johnson and Plank (1999) and Balzer (1999).

Table DR2

Sample	LAR 1M	LAR 2	ZAR 12	ZAR 1	ZAR 2	ZAR 3	ZAR 5	ZAR 7	ZAR 6	ZAR 8	ZAR 9
Split											
UTM E	544.9	544.7	557.5	561.1	561.1	562.2	570.3	577.1	574	578	582.5
UTM N	1405.1	1405.7	1402.4	1400	1400.1	1400.1	1406.6	1410.7	1406.9	1410.6	1409.5
Age (Ma)	7.96			7.7						16.72 *	
err	0.1			0.11						0.25	
Age gr.	I	I	I	I	I	I	II	II	II	II	II
Region	Lar	Lar	Zar	Zar	Zar	Zar	Zar	Zar	Zar	Zar	Zar
Dist. (km)	657	657	669	673	673	673	675	678	678	680	683
DCP-ES:											
SiO2	67.72	57.21	68.94	57.95	51.83	60.60	50.85	51.80	65.71	60.86	65.51
TiO2	0.55	0.75	0.81	0.90	0.95	1.11	0.85	1.10	0.85	0.85	0.82
Al2O3	16.59	18.23	15.09	19.13	20.20	15.96	18.72	19.10	15.86	17.97	16.15
FeO	3.89	7.30	4.24	6.85	9.21	7.60	9.58	8.38	4.60	5.56	4.73
MnO	0.06	0.15	0.05	0.17	0.17	0.15	0.19	0.19	0.10	0.12	0.11
MgO	0.63	3.96	0.48	2.27	3.24	2.60	5.73	2.63	1.27	1.95	1.45
CaO	3.76	8.11	2.82	6.97	10.74	6.92	10.79	12.67	3.99	6.00	4.12
Na2O	4.58	2.96	4.66	4.39	2.90	2.76	2.63	3.01	3.77	4.16	4.03
K2O	2.04	1.18	2.66	1.02	0.56	1.98	0.54	0.78	3.55	2.17	2.77
P2O5	0.16	0.15	0.24	0.34	0.21	0.31	0.12	0.35	0.29	0.37	0.30
LOI	1.19	1.97	1.30	1.45	1.37	2.42	1.44	7.03	2.14	1.28	2.06
ICP-MS:											
Li			15.07	6.75				21.81	27.07		27.75
Be			1.42	1.06				0.76	1.47		1.42
Sc	14.24	28.85	18.36	23.43	30.22	27.98	34.30	24.42	15.45	19.21	15.16
V	76.88	227.30	40.67	130.92	174.54	193.31	301.04	211.65	72.79	108.35	85.11
Cr		9.80	0.93	1.50	33.72	8.23	35.48	26.66	1.37	0.62	1.55
Co	6.40	23.75	3.79	13.50	24.22	15.16	35.16	23.03	7.16	11.55	7.69
Ni	0.55	25.30	0.47	2.97	14.16	13.45	28.30	16.15	2.25	15.33	2.48
Cu	31.66	118.13	10.75	14.62	144.00	69.75	152.67	65.36	25.65	36.28	19.53
Zn	55.66	76.32	90.50	85.56	72.34	107.55	80.40	79.27	69.13	63.42	71.67
Rb	43.14	20.05	57.18	16.66	11.66	41.81	7.37	16.46	90.08	49.13	64.97
Sr	314.53	383.80	297.48	580.55	502.43	372.06	390.27	655.74	310.76	383.24	343.76
Y	41.29	22.91	63.77	30.52	23.41	34.38	15.15	24.40	41.72	31.93	46.47
Zr	165.90	76.70	234.19	90.73	58.93	140.48	48.38	104.84	246.42	165.25	238.87
Nb	3.35	1.49	4.39	2.21	1.45	3.25	0.93	2.51	5.48	4.18	5.27
Cs	1.16	1.39	1.69	0.45	0.38	3.07	0.08	1.70	2.15	1.31	0.63
Ba	1293.25	619.32	1606.50	723.67	485.50	1020.42	266.47	470.91	1039.23	645.71	939.50
Ga			11.30	17.07				17.53	9.38		11.14
La	19.47	4.92	17.74	9.88	7.11	10.85	3.53	8.74	16.96	13.19	17.06
Ce	35.63	12.32	39.21	22.46	14.95	25.96	8.96	20.91	39.29	31.19	39.15
Pr	6.90	2.03	7.24	3.80	2.72	4.23	1.49	3.21	5.82	4.70	5.89
Nd	29.69	9.76	33.33	17.85	12.99	19.77	7.38	14.76	25.20	20.94	25.66
Sm	7.10	2.85	8.54	4.69	3.51	5.21	2.19	3.79	6.25	5.18	6.47
Eu	1.77	0.94	2.13	1.65	1.28	1.51	0.84	1.22	1.55	1.46	1.67
Gd	7.25	3.39	9.69	5.25	4.13	5.85	2.65	4.24	6.62	5.49	7.16
Tb	1.28	0.64	1.73	0.91	0.72	1.06	0.48	0.73	1.17	0.98	1.23
Dy	7.07	3.71	10.04	5.10	4.10	5.82	2.78	4.06	6.59	5.33	6.94
Ho	1.44	0.81	2.15	1.06	0.88	1.24	0.60	0.84	1.39	1.11	1.46
Er	4.11	2.28	6.22	2.96	2.46	3.47	1.65	2.32	3.93	3.10	4.05
Yb	4.05	2.32	6.20	2.84	2.36	3.40	1.60	2.16	3.88	3.02	3.81
Lu	0.65	0.37	0.98	0.45	0.37	0.54	0.25	0.34	0.62	0.47	0.61
Hf	4.33	2.27	6.44	2.43	1.72	4.10	1.44	2.77	6.21	4.48	6.01
Ta	0.22	0.10	0.30	0.14	0.10	0.20	0.07	0.18	0.38	0.28	0.36
Pb	5.66	3.57	8.68	2.30	2.40	6.42	2.24	4.51	9.15	6.72	8.22
Th	2.15	0.81	2.34	0.98	0.62	1.57	0.41	1.37	3.56	2.50	3.45
U	1.01	0.42	1.10	0.42	0.28	0.74	0.19	0.57	1.53	1.09	1.50
$^{87}Sr/^{86}Sr$	0.703785			0.703796							

Table DR2

Sample	ZAR 11	CD 1	CD 2	CDC 2	CDC 3	LM 3B	LM 3A	LM 2A	LM 2B	LM 1	SJ 2
Split				Ny	Ny						
UTM E	582.3	594.5	595.8	602.8	602.9	599.2	599.2	600.5	600.5	602.5	610.4
UTM N	1408.1	1400.8	1401.6	1394.6	1394.6	1388.4	1388.4	1388.62	1388.62	1377.8	1361.9
Age (Ma)											
err											
Age gr.	II	I	I	I	I	I	I	I	I	I	I
Region	Zar	CD-LM	CD-LM	CD-LM	CD-LM	CD-LM	CD-LM	CD-LM	CD-LM	CD-LM	SJ-LL
Dist. (km)	683	697	697	708	708	709	709	711	711	718	735
DCP-ES:											
SiO2	66.21	52.44	51.46	53.30	51.97	53.92	51.64	50.00	50.06	52.10	51.84
TiO2	0.85	0.87	1.13	0.81	0.81	1.44	1.05	1.08	0.84	0.99	0.92
Al2O3	15.62	19.98	18.86	16.56	20.34	17.29	17.92	19.70	23.32	17.73	17.83
FeO	4.73	9.06	10.45	9.08	8.22	11.29	9.33	10.87	7.73	9.42	8.84
MnO	0.10	0.18	0.30	0.17	0.16	0.19	0.17	0.18	0.14	0.19	0.23
MgO	1.35	3.25	3.97	6.87	4.79	3.31	5.95	3.84	2.72	6.38	6.18
CaO	3.85	10.78	9.71	9.68	10.35	7.87	9.88	10.40	11.92	9.26	10.33
Na2O	3.93	2.73	3.14	2.87	2.88	3.51	3.01	3.00	2.69	2.92	2.81
K2O	3.03	0.58	0.71	0.49	0.40	0.80	0.74	0.69	0.42	0.68	0.72
P2O5	0.32	0.13	0.27	0.17	0.10	0.37	0.30	0.24	0.16	0.33	0.29
LOI	3.47	1.15	1.02	0.54	0.52	2.39	0.72	0.92	0.73	0.48	0.89
ICP-MS:											
Li	24.66	6.43									
Be	1.49	0.65									
Sc	16.05	33.46	31.40	31.84	26.46	33.23	28.73	30.55	23.20	32.16	33.60
V	69.41	304.86	294.78	232.31	227.10	270.75	221.89	335.49	232.37	237.16	255.63
Cr	0.84	28.14	10.24	310.65	63.33	2.88	173.39	7.40	4.20	180.65	301.53
Co	6.91	31.25	35.34	36.72	32.23	23.23	34.14	31.48	21.69	36.73	37.48
Ni	1.88	14.81	13.53	98.20	53.09	9.30	80.92	27.70	10.09	73.97	74.41
Cu	18.99	156.55	156.69	102.50	100.91	189.66	101.70	175.30	102.06	110.31	109.13
Zn	71.33	78.60	92.32	79.21	65.46	118.26	86.83	78.00	61.30	98.09	82.22
Rb	71.53	13.39	13.71	6.47	4.54	16.53	9.96	11.76	7.92	8.55	8.41
Sr	254.47	482.79	482.80	444.31	525.03	456.76	435.14	631.08	553.01	445.21	505.33
Y	41.10	21.06	55.29	25.85	21.42	35.96	22.55	22.31	16.49	24.78	24.84
Zr	249.56	53.78	71.14	46.05	43.56	99.01	91.24	53.11	38.65	89.24	65.84
Nb	5.57	1.20	2.74	1.60	1.53	3.81	4.28	2.03	1.45	3.72	2.44
Cs	1.63	0.45	0.42	0.26	0.18	0.71	0.24	0.40	0.23	0.22	0.18
Ba	1066.93	579.77	1990.53	669.98	484.45	763.04	690.30	579.28	501.01	601.41	795.60
Ga	10.41	16.58									
La	17.26	8.06	15.06	6.09	4.56	11.82	9.25	7.18	5.07	9.91	9.28
Ce	39.99	16.47	29.37	13.06	10.37	22.26	20.36	15.82	9.81	20.97	20.61
Pr	5.94	2.78	4.83	2.15	1.77	4.29	3.11	2.68	1.75	3.25	3.29
Nd	25.68	12.49	22.92	10.40	8.71	20.59	14.16	12.87	8.37	14.60	15.46
Sm	6.33	3.33	6.10	2.88	2.49	5.55	3.59	3.38	2.30	3.61	3.98
Eu	1.58	1.06	2.15	1.14	0.98	1.80	1.29	1.21	0.96	1.20	1.44
Gd	6.70	3.76	7.76	3.75	3.21	6.46	4.00	3.80	2.77	4.06	4.54
Tb	1.19	0.67	1.36	0.67	0.58	1.13	0.71	0.67	0.49	0.70	0.78
Dy	6.64	3.75	7.82	3.93	3.31	6.29	3.99	3.69	2.79	4.01	4.36
Ho	1.39	0.79	1.73	0.86	0.72	1.32	0.83	0.78	0.60	0.83	0.92
Er	3.90	2.16	4.91	2.44	2.03	3.68	2.32	2.17	1.70	2.36	2.56
Yb	3.86	2.09	4.46	2.33	1.87	3.46	2.19	2.02	1.60	2.25	2.45
Lu	0.62	0.33	0.73	0.37	0.30	0.54	0.34	0.32	0.25	0.36	0.39
Hf	6.24	1.52	2.03	1.31	1.23	2.75	2.36	1.63	1.18	2.24	1.78
Ta	0.38	0.08	0.18	0.11	0.10	0.24	0.26	0.12	0.10	0.22	0.15
Pb	10.40	2.75	3.12	2.17	1.86	4.20	3.16	2.72	1.94	3.62	2.95
Th	3.64	0.54	0.77	0.50	0.16	1.06	0.49	0.55	0.35	0.46	0.51
U	1.55	0.23	0.35	0.20	0.07	0.40	0.21	0.26	0.14	0.20	0.23
$^{87}Sr/^{86}Sr$									0.703641		

Table DR2

Sample	SJ 3	EC 136	LL 3	LL 4	EC 177	EC 179	LL 1	LL 6	LL 5	LL 2	SLU 2
Split		Ny			Ny	Ny					Ny
UTM E	610.4	616.9	622.1	622.4	622.2	622.2	618.4	641.5	647.5	620.5	649
UTM N	1361.9	1365.6	1368	1369.3	1373.1	1373.2	1365.7	1367.7	1341.6	1366	1388.5
Age (Ma)							8.87		11.23	10.16	
err							0.21		0.24	0.26	
Age gr.	I	I	I	I	I	I	I	I	I	I	II
Region	SJ-LL	SJ-LL	SJ-LL	SJ-LL	SJ-LL	SJ-LL	SJ-LL	SJ-LL	SJ-LL	SJ-SL	SL
Dist. (km)	735	737	740	740	740	740	740	754	777	740	748
DCP-ES:											
SiO2	63.18	56.70	59.79	49.59	50.73	53.17	48.85	51.55	52.20	49.74	55.75
TiO2	0.62	0.92	0.73	1.03	1.02	1.00	0.74	1.02	0.82	0.87	0.89
Al2O3	17.84	18.17	17.51	18.41	17.82	16.68	15.77	19.27	17.84	16.86	18.73
FeO	5.07	8.00	6.88	11.00	10.04	9.51	9.54	9.12	8.75	9.29	7.75
MnO	0.15	0.17	0.14	0.20	0.20	0.17	0.18	0.21	0.17	0.17	0.18
MgO	1.42	2.53	3.16	5.73	5.54	5.70	10.25	3.71	5.74	8.82	3.58
CaO	4.93	8.28	6.91	10.37	10.84	9.50	12.05	11.24	10.52	10.72	8.30
Na2O	4.31	3.65	3.02	2.72	2.72	2.97	1.93	2.78	2.58	2.52	3.72
K2O	2.24	1.25	1.67	0.75	0.77	0.84	0.52	0.86	1.18	0.72	0.72
P2O5	0.25	0.33	0.18	0.19	0.32	0.47	0.17	0.25	0.19	0.28	0.39
LOI	1.13	0.65	1.79	1.15	0.93	0.85	1.70	1.06	0.29	1.48	1.43
ICP-MS:											
Li	9.88	6.26	5.32				5.04				4.35
Be	1.30	0.79	0.83				0.52				1.14
Sc	12.55	27.81	23.71	35.17	34.86	31.61	39.93	33.15	36.56	31.94	20.41
V	122.06	227.27	192.52	357.45	296.29	236.10	268.74	294.97	267.00	241.54	178.18
Cr	2.23	2.08	15.90	15.53	162.72	169.56	391.30	16.76	110.81	315.80	2.22
Co	12.85	20.39	20.01	36.21	43.33	30.56	44.46	27.12	34.18	39.77	21.18
Ni	4.43	3.00	10.69	26.37	76.38	73.56	109.62	26.69	40.96	95.54	3.91
Cu	45.86	129.83	88.13	219.94	151.43	116.04	120.73	201.60	134.91	135.01	59.44
Zn	67.11	84.83	75.08	91.52	79.83	82.12	71.63	88.67	87.22	80.99	84.25
Rb	48.64	20.86	39.80	21.64	10.88	9.77	9.36	16.04	26.73	12.04	23.88
Sr	486.11	522.38	417.97	570.86	540.44	506.51	453.71	456.00	409.86	513.79	693.45
Y	26.47	25.13	24.74	18.50	18.75	24.03	14.34	24.10	20.42	17.95	27.01
Zr	161.71	87.10	112.72	41.67	50.10	78.28	38.49	73.29	76.85	56.95	120.00
Nb	3.14	2.00	2.32	0.99	1.77	3.14	1.24	3.07	2.85	2.46	3.38
Cs	0.76	0.52	1.64	0.19	0.31	0.15	0.06	0.60	0.78	0.26	1.54
Ba	1447.14	877.84	997.51	267.38	706.92	546.36	249.19	595.19	717.22	414.94	488.05
Ga	9.13	21.18	12.82				12.89				19.38
La	15.25	7.44	8.81	5.80	6.59	9.16	5.19	7.21	7.97	7.67	12.26
Ce	31.49	17.42	19.76	14.11	14.34	19.88	12.28	17.06	17.60	18.15	27.48
Pr	4.69	2.82	3.07	2.41	2.32	3.21	2.00	2.75	2.77	2.87	4.21
Nd	19.65	13.25	13.81	11.62	10.58	14.46	9.32	13.05	12.60	13.34	18.58
Sm	4.52	3.60	3.52	3.10	2.79	3.64	2.44	3.56	3.27	3.33	4.55
Eu	1.39	1.23	1.08	1.13	1.07	1.30	0.88	1.19	1.11	1.16	1.45
Gd	4.53	4.10	3.93	3.37	3.23	4.14	2.75	4.16	3.66	3.57	4.74
Tb	0.77	0.74	0.71	0.59	0.56	0.73	0.48	0.76	0.66	0.61	0.81
Dy	4.23	4.18	3.99	3.27	3.20	4.12	2.62	4.19	3.60	3.24	4.49
Ho	0.87	0.87	0.84	0.68	0.67	0.85	0.53	0.89	0.75	0.66	0.92
Er	2.49	2.47	2.40	1.88	1.86	2.43	1.45	2.49	2.10	1.80	2.57
Yb	2.54	2.45	2.42	1.79	1.77	2.36	1.36	2.45	2.05	1.72	2.57
Lu	0.42	0.38	0.39	0.28	0.28	0.38	0.21	0.39	0.32	0.27	0.40
Hf	3.91	2.34	3.03	1.32	1.30	1.95	1.12	2.14	2.17	1.56	2.88
Ta	0.21	0.13	0.17	0.06	0.12	0.18	0.08	0.19	0.18	0.14	0.22
Pb	5.64	3.17	5.22	1.97	2.15	2.84	1.65	3.40	3.16	2.79	4.24
Th	1.80	1.13	1.47	0.31	0.64	0.48	0.32	0.89	1.19	0.43	1.64
U	1.00	0.51	0.66	0.19	0.29	0.22	0.15	0.40	0.53	0.23	0.68
$^{87}Sr/^{86}Sr$							0.703793				

Table DR2

Sample	SL 1	SL 2	SE 1	SE 2	JUI 1	JUI 2	RAMA 16	RAM 16	RAMA 15	RAM 15C
Split							Ny		Ny	
UTM E	644.4	647.7	666.5	672.3	685.2	690	699.7	699.6	702.2	702.39
UTM N	1368.7	1361.9	1341.6	1341.3	1333.5	1329.3	1327.5	1327.5	1330.9	1330.99
Age (Ma)	15.95 *		17.58					23.89		19.66
err	0.46		0.26					0.88		0.38
Age gr.	II	II	II	II	II	II	II	II	II	II
Region	SL	SL	SE-Rama	SE-Rama	SE-Rama	SE-Rama	SE-Rama	SE-Rama	SE-Rama	SE-Rama
Dist. (km)	755	763	792	794	810	818	825	825	826	826
DCP-ES:										
SiO2	54.45	67.00	52.38	50.25	50.05	66.65	52.26	52.33	50.72	49.83
TiO2	1.02	0.56	0.82	0.97	0.90	0.50	0.86	0.84	0.85	0.69
Al2O3	18.16	16.08	19.76	18.25	19.28	15.99	17.66	18.38	20.52	22.26
FeO	9.42	3.84	8.20	9.59	9.81	3.89	8.85	8.69	8.80	7.68
MnO	0.19	0.11	0.15	0.18	0.18	0.12	0.14	0.12	0.18	0.14
MgO	4.08	1.43	4.32	5.99	4.99	1.97	6.72	6.04	5.01	4.36
CaO	8.46	4.00	10.59	11.61	11.88	5.00	9.76	9.96	10.88	12.55
Na2O	3.20	3.82	2.86	2.47	2.45	3.93	2.80	2.70	2.46	2.09
K2O	0.83	2.98	0.71	0.49	0.31	1.84	0.78	0.72	0.44	0.28
P2O5	0.20	0.20	0.20	0.19	0.15	0.09	0.19	0.22	0.14	0.11
LOI	1.16	5.02	1.16	2.99	1.21	0.94	0.91	2.29	0.60	0.62
ICP-MS:										
Li	4.16	6.85	5.33					4.75	5.41	
Be	0.72	1.26	0.66					0.65	0.35	
Sc	35.66	11.07	30.62	35.36	35.83	17.11	29.77	30.63	32.83	28.48
V	302.96	74.79	252.63	288.41	309.42	111.65	240.41	231.44	294.56	248.72
Cr	13.93	4.63	45.43	50.81	35.70	14.18	138.18	139.90	28.43	19.95
Co	28.54	7.24	27.32	33.15	31.68	12.94	34.13	32.78	31.50	27.55
Ni	10.48	3.35	36.35	26.86	36.15	13.29	59.71	58.99	17.58	30.79
Cu	95.76	27.05	66.53	130.75	138.62	41.04	77.58	98.34	93.89	156.24
Zn	92.78	59.82	80.41	76.93	77.72	52.32	73.29	70.83	75.22	65.11
Rb	48.95	62.06	11.28	3.85	2.49	32.70	23.13	10.77	4.70	4.11
Sr	413.97	333.85	524.52	442.26	441.07	268.36	463.00	469.28	415.44	408.52
Y	25.61	23.30	19.57	16.19	16.17	20.90	17.42	17.24	14.86	11.74
Zr	92.31	168.70	57.41	49.99	35.31	128.25	60.20	58.30	36.81	29.59
Nb	2.25	3.89	1.63	1.63	0.96	2.54	4.75	2.46	0.76	0.69
Cs	0.82	0.49	0.07	0.49	0.06	0.39	0.28	0.07	0.05	0.13
Ba	383.58	1324.39	343.92	237.17	220.62	705.89	282.12	277.80	168.43	143.67
Ga	17.44	9.26	17.17					15.56	18.66	
La	7.42	14.01	6.30	5.78	4.06	9.16	12.11	6.68	3.06	2.78
Ce	17.51	28.94	14.59	13.70	9.71	20.35	28.19	15.23	7.53	6.81
Pr	2.79	4.03	2.32	2.19	1.63	2.93	4.49	2.38	1.27	1.15
Nd	12.98	16.35	10.88	10.37	7.98	12.45	20.67	10.75	6.28	5.66
Sm	3.54	3.71	2.88	2.79	2.33	2.97	5.45	2.73	1.85	1.63
Eu	1.13	1.11	1.04	1.03	0.90	0.96	1.62	0.98	0.73	0.65
Gd	4.05	3.78	3.22	3.15	2.73	3.17	6.38	3.01	2.23	1.93
Tb	0.73	0.65	0.57	0.56	0.50	0.58	1.13	0.53	0.42	0.36
Dy	4.22	3.66	3.20	3.13	2.92	3.32	6.54	2.96	2.40	2.06
Ho	0.90	0.77	0.68	0.65	0.62	0.71	1.37	0.61	0.52	0.45
Er	2.54	2.24	1.90	1.82	1.73	2.12	3.86	1.71	1.47	1.25
Yb	2.50	2.41	1.84	1.75	1.69	2.34	3.70	1.65	1.46	1.23
Lu	0.39	0.39	0.29	0.27	0.26	0.38	0.58	0.26	0.23	0.20
Hf	2.52	4.03	1.58	1.48	1.11	3.35	3.47	1.56	1.03	0.92
Ta	0.16	0.29	0.11	0.11	0.06	0.21	0.32	0.16	0.05	0.05
Pb	3.03	8.12	2.02	2.05	1.75	4.37	3.73	2.03	1.11	0.62
Th	1.18	2.65	0.69	0.58	0.43	1.92	1.97	0.46	0.32	0.28
U	0.51	1.19	0.32	0.24	0.21	0.90	0.78	0.23	0.14	0.14
$^{87}Sr/^{86}Sr$	0.703604									

Table DR2

Sample	RAMA 14	RAMA 11	RAMA 10	RAMA 7
Split	Ny	Ny	Ny	Ny
UTM E	717.4	738.3	749.6	756.4
UTM N	1333.7	1326.2	1327.4	1329.9
Age (Ma)				
err				
Age gr.	II	II	II	II
Region	SE-Rama	SE-Rama	SE-Rama	SE-Rama
Dist. (km)	836	856	864	867
DCP-ES:				
SiO2	53.89	60.72	50.59	50.89
TiO2	1.49	0.87	0.99	1.07
Al2O3	15.51	17.28	17.26	17.69
FeO	11.45	6.63	9.18	9.33
MnO	0.20	0.15	0.20	0.21
MgO	4.28	2.51	8.23	7.21
CaO	8.43	6.18	10.21	9.77
Na2O	3.12	4.21	2.46	2.89
K2O	1.23	1.25	0.61	0.67
P2O5	0.39	0.20	0.27	0.28
LOI	0.49	0.62	1.19	0.68
ICP-MS:				
Li		9.25		
Be		0.96		
Sc	43.91	23.86	32.32	32.70
V	443.19	165.87	248.52	247.41
Cr	15.81	3.30	205.24	242.92
Co	35.85	15.73	38.73	36.50
Ni	15.45	2.96	92.76	92.05
Cu	294.28	39.99	201.59	81.60
Zn	115.87	95.07	73.55	75.85
Rb	9.31	20.27	9.99	8.66
Sr	335.52	432.04	338.92	379.07
Y	38.69	30.70	17.62	20.23
Zr	126.43	96.54	52.28	67.38
Nb	2.56	3.33	4.20	3.13
Cs	0.06	0.18	0.07	0.05
Ba	483.64	492.64	172.86	232.64
Ga		20.60		
La	6.96	8.82	5.84	6.43
Ce	15.83	20.23	13.44	15.02
Pr	2.46	3.24	2.10	2.38
Nd	11.15	15.09	9.66	10.92
Sm	2.83	4.08	2.59	2.89
Eu	1.03	1.44	0.95	1.07
Gd	3.20	4.67	3.07	3.44
Tb	0.56	0.84	0.55	0.61
Dy	3.12	4.86	3.11	3.49
Ho	0.65	1.03	0.65	0.74
Er	1.81	2.96	1.84	2.08
Yb	1.77	2.99	1.78	2.04
Lu	0.28	0.47	0.28	0.32
Hf	1.63	2.49	1.45	1.76
Ta	0.17	0.22	0.26	0.21
Pb	1.93	2.70	1.46	1.55
Th	0.48	1.03	0.53	0.55
U	0.24	0.50	0.22	0.23
$^{87}Sr/^{86}Sr$				

Table DR3. Bulk sediment calculations

	Hemi-1	Carb-1	Carb-2	Carb-3	Bulk-2.5	Bulk-12
Thick (m)					464	454
dens(g/cc)	1.37	1.72	1.92	1.54	1.64	1.69
SiO2	55.00	13.60	4.25	29.67	19.58	15.54
TiO2	0.592	0.030	0.021	0.344	0.135	0.101
Al2O3	12.36	0.880	0.160	7.19	2.92	2.21
Fe2O3	6.21	3.14	1.97	5.02	3.49	3.35
MnO	0.146	0.610	0.230	0.434	0.444	0.495
MgO	2.26	0.980	0.781	1.71	1.18	1.11
CaO	2.99	41.3	52.2	27.6	36.2	40.2
NaO	2.10	0.430	0.196	1.06	0.700	0.532
K2O	1.82	0.260	0.169	1.02	0.539	0.419
P2O5	0.126	0.153	0.130	0.157	0.143	0.150
LOI	16.4	38.6	40.0	25.9	34.7	35.9
H20-	61	44	31	52	46	44
CaCO3 %	0.0	73.8	90.9	45.9	63.2	70.6
Sc	14.8	3.67	2.20	9.98	5.49	4.86
V	117	74.5	48.7	118	77.4	79.5
Cr	35.1	11.5	17.5	29.0	17.2	16.7
Co	58.1	6.60	4.15	14.4	15.9	7.95
Ni	181	39.9	26.1	38.5	63.9	36.9
Cu	152	139	61.9	121	126	120
Zn	227	69.7	31.0	75.8	91.7	63.6
Rb	39.7	6.40	4.54	35.0	12.4	12.7
Sr	332	1290	1523	926	1155	1250
Y	27.7	27.1	12.8	25.8	24.3	24.0
Zr	138	19.4	3.52	62.9	38.8	26.5
Nb	3.92	0.878	0.249	4.432	1.329	1.586
Cs	2.25	0.257	0.155	2.811	0.616	0.834
Ba	3344	2785	1875	1988	2705	2422
La	20.7	14.2	7.4	16.7	14.0	13.5
Ce	28.3	5.13	1.43	19.89	8.79	7.86
Pr	4.80	2.60	1.40	3.65	2.77	2.61
Nd	18.3	10.1	5.2	14.0	10.7	10.1
Sm	4.12	2.48	1.08	3.11	2.50	2.35
Eu	1.07	0.492	0.250	0.705	0.553	0.495
Gd	4.38	2.63	1.29	3.11	2.69	2.48
Tb	0.700	0.480	0.240	0.548	0.473	0.449
Dy	4.49	3.16	1.61	3.42	3.10	2.92
Ho	1.00	0.670	0.365	0.739	0.670	0.627
Er	2.91	1.80	1.05	2.03	1.86	1.71
Yb	2.68	1.57	1.00	1.85	1.67	1.53
Lu	0.400	0.230	0.155	0.281	0.247	0.227
Hf	2.74	0.297	0.054	1.377	0.712	0.502
Ta	0.205	0.046	0.013	0.285	0.070	0.096
Pb	9.03	5.85	3.61	7.73	5.99	5.85
Th	2.94	0.381	0.088	2.893	0.809	0.911
U	5.47	0.159	0.169	0.766	1.174	0.303
87Sr/86Sr	0.70763	0.70866	0.70831	0.70840	0.70851	0.70824

Sedimentary column compositions calculated based on the section at Site 495, which consists of hydrothermal -oxide-carbonate (Carb-2), overlain by pelagic carbonate with opal (Carb-1), hemipelagic diatom ooze, and hemipelagic ooze with arc ash (Hemi-1). These same units are used to calculate the 2.5 Ma column (see below), but assuming 2.5 Ma (~27 m) more Carb-1 preceding the carbonate crash, and 2.5 Ma (~ 27 m) less of Hemi-1 immediately following the crash, based on accumulation rates in Aubouin et al. (1982). The top unit in the 12 Ma column (Carb-3) was assumed to be deposited prior to both the carbonate crash and the Costa Rica dome, but with otherwise a similar sedimentation history to Hemi-1 in Site 495.

Hemi-1 = average of top 5 samples (145 m) at Site 495 (Patino et al., 2000). Co calculated from Co/Fe, Zn from Zn/Cu, Ga from Ga/Al, Zr from Zr/Al, Hf from Hf/Zr, and Ta from Nb/Ta in 844 and 845 sediments (Table DR1).

Carb-1 = sample s24-7-19 in Patino et al, (2000), which has ~75% CaCO3, appropriate to the average for the unit. Other elements calculated as above.

Carb-2 = average of lower 7 samples (63 m) at Site 495 (Patino et al., 2000), where Fe2O3/Al2O3 > 7, indicative of hydrothermal particulates. Other elements calculated as above.

Carb-3 = calculated based on opal-free accumulation rates in Site 495 as 35 m arc ash (the average of all Nicaraguan volcanics with < 40 ppm Cr in the Centam database; Carr and Rose, 1987), 35 m continental detritus (post-Archean average shale; Taylor and McLennan, 1985); and 65 m carbonate (as in Carb-1, above).

2.5 Ma sedimentary column = 140m Hemi1 + 255m Carb1 + 63m Carb2.

12 Ma sedimentary column = 136m Carb-3 + 255m Carb1 + 63m Carb2.

Bulk calculations are by mass, based on the thickness, wet bulk density and H2O- of each unit.

References to Data Reposity Items

Aubouin, J. and von Huene, R., 1982, Initial Reports of the Deep Sea Drilling Project , Volume 67: Washington, D.C., U.S., Government Printing Office, 799 p.

Balzer, V.G., 1999, The late Miocene history of sediment subduction and recycling as recorded in the Nicaraguan volcanic arc [M.S. thesis]: Lawrence, University of Kansas, 151 p.

Carr, M.J., and Rose, W.I., Jr., 1987, CENTAM—A data base of Central American volcanic rocks: Journal of Volcanology and Geothermal Research, v. 33, p. 239–240.

Johnson, M.C., and Plank, T., 1999, Dehydration and melting experiments constrain the fate of subducted sediments: Geochemistry Geophysics and Geosystems, v. 1, p. 1999GC000014.

Mayer, L., Pisias, N., and Janacek, T., 1992, Proceedings of the Ocean Drilling Program, Initial reports, Volume 138: College Station, Texas, Ocean Drilling Program, 855 p.

Nyström, J-O., Levi, B., Troeng, B., Ehrenborg, J., and Carranza, G., 1998, Geochemistry of volcanic rocks in a traverse through Nicaragua: San Jose, Costa Rica, Revista Geologica de America Central, v. 8, p. 77–109.

Patino, L.C., Carr, M.J., and Feigenson, M.D., 2000, Local and regional variations in Central American arc lavas controlled by variations in subducted sediment input: Contributions to Mineralogy and Petrology, v. 138, p. 265.

Plank, T., and Ludden, J.N., 1992, Geochemistry of sediments in the Argo Abyssal Plain at ODP Site 765: A continental margin reference section for sediment recycling in subduction zones, *in* Ludden, J.N., and Gradstein, F., et al., Proceedings of the Ocean Drilling Program, Scientific results, Volume 123: College Station, Texas, Ocean Drilling Program, p. 167–189.

Taylor, S.R., and McLennan, S.M., 1985, The continental crust: Its composition and evolution: Oxford, Blackwell, 312 p.